Scaling Behavior of Cohesive Self-Gravitating Aggregates

Emilien Azéma,[1,*] Paul Sánchez,[2,†] and Daniel J. Scheeres[3,‡]

[1] *LMGC, Univ. Montpellier, CNRS, Montpellier, France.*
[2] *Colorado centre for Astrodynamics Research, University of Colorado Boulder, 431 UCB, Boulder, CO 80309*
[3] *Aerospace Engineering Department, University of Colorado Boulder, Boulder, 429 UCB, CO 80309*

(Dated: August 3, 2018)

By means of extensive three dimensional Contact Dynamics simulations, we analyse the strength properties and microstructure of a granular asteroid, modeled as a self-gravitating cohesive granular aggregates composed of spherical particles, and subjected to diametrical compression tests. We show that, for a broad range of system parameters (shear rate, cohesive forces, asteroid diameter), the behaviour can be described by a modified inertial number that incorporates inter-particle cohesion and gravitational forces. At low inertial numbers, the behaviour is ductile with a well defined stress peak that scales with internal pressure with a pre-factor $\simeq 0.9$. As the inertial number increases, both, the pre-factor and fluctuations around the mean, increase, evidencing a dynamical crisis resulting from the destabilizing effect of particle inertia. From a micro-mechanical description of the contact and force networks, we propose a model that accounts for solid fraction, local stress, particle connectivity and granular texture. In the limit of small inertial numbers, we find a very good agreement of the theoretical estimate of compressive strength, evidencing the major role of these structural parameters for the modelled aggregates.

PACS numbers: 96.30.Ys, 81.05.Rm, 83.80.Fg

Understanding the physical and mechanical properties of small planetary bodies (comets, asteroids, small satellites) is essential not only for the study of the Solar System and its origins, but also as a basis for future space exploration and mining missions [1]. Until very recently, it was assumed that the smallest of asteroids were monolithic rocks with a bare surface [2, 3], but recent space missions and observations have established that not only their surfaces are covered by regolith, but that their internal structure is not monolithic either [4–6]. From these observations, the concept of "Granular Asteroid" has progressively emerged [7, 8].

Granular asteroids are naturally occurring gravitational aggregates (rubble piles) bound together by gravitational and possibly cohesive forces. They have large interior voids which allow them to support large plastic deformations [9]. Their macroscopic behaviour and internal structure are still not well known and how to predict their mechanical strength, based on their microstructure and dynamics, is still an open question [1, 10]. However, in view of their discrete nature, it is reasonable to use the theoretical concepts and numerical tools developed for granular media to study them.

After more than fifteen years of research, the two following general features have been well established for granular materials (with some caveats for real geological systems [11]): (1) their dynamical behaviour, under various boundary conditions and confining geometries, is well captured through the so-called *inertial number* I, defined as the ratio of the particle relaxation time $d\sqrt{\rho_0/p}$, under a confining stress p and for a particle of density ρ_0 and diameter d, to shear time $t_s = \dot{\gamma}^{-1}$ imposed by the shear rate $\dot{\gamma}$ [12–14] and, (2) their strength properties result from the buildup of anisotropic structures at the particle scale which are induced by steric effects, force transmission and friction mobilisation [15–18].

In granular asteroids, long-range gravitational forces have to be taken into account along with cohesive forces and so, the generalisation of these "granular concepts" is highly non-trivial. However, some recent simulations have started to include these effects; this has led researchers to propose new microscopic mechanisms [19, 20] to explain the behaviour of some of the small members of the Near Earth Object (NEO) population. For example, the fact that small asteroids (< 150 m) can have a rotation rate higher than what a purely gravitational model would predict [21] can be attributed to local cohesion [22–24], where the smallest particles agglomerate in the form of a weak cohesive matrix that binds the larger particles [19, 20]. Unfortunately, a general framework for the analysis of such bodies is still lacking. In this letter we lay the foundation of a framework that unifies the I-rheology with the overburden pressure given by self-gravity.

Considering that several forces come into play [19], it may be assumed that internal stresses result from two characteristic stresses acting on particles: 1) inter-particle tensile strength $\eta = f_0/d^2$, where f_0 is the cohesive force, and 2) interior stress given by $\mathcal{P}(r) = 0.25\rho_0 g_0 D(1 - 4r^2/D^2)$, with $g_0 = GM_a/D^2$ where G is the gravitational constant, M_a and D the total mass and diameter of the asteroid, r the distance from the centre, assuming a constant bulk density and spherical geometry. The pressure at the centre is given by $P_0 = \rho_0 g_0 D/4$ and can be used as a referential interior stress. Two different particle relaxation times can be built as $t_\eta = d\sqrt{\rho_0/\eta}$ and

*Electronic address: emilien.azema@umontpellier.fr
†Electronic address: diego.sanchez-lana@colorado.edu
‡Electronic address: daniel.scheeres@colorado.edu

$t_{g_0} = d\sqrt{\rho_0/P_0}$, leading, in combination with t_s, to the definition of two dimensionless numbers: $I_\eta = \dot{\gamma} d\sqrt{\rho_0/\eta}$ and $I_{g_0} = \dot{\gamma} d\sqrt{\rho_0/P_0}$. From these two numbers, we can also find a modified version of the *Bond Number*: $\lambda = \eta/P_0 = (I_{g_0}/I_\eta)^2$, which has been originally defined as the ratio of cohesive to gravitational forces [19, 25]. We thus expect that the rheology of a granular asteroid will be governed by two of these three numbers.

By means of extensive 3D Contact Dynamics simulations [26–28][49], we analyse the stress-strain behavior and microstructure of a granular asteroid, modelled as a cohesive granular agglomerate of spherical particles, subjected to vertical compression together with gravitational forces and for a broad range of parameters I_η, I_{g_0} and η. As we shall see, the peak strength, as well as the microstructure, scale with a modified inertial number that, in fact, combines two of these three numbers, so extending the *granular paradigm* to these ideal self-gravitating systems.

First, we build a large sample of 10 000 spherical particles under isotropic compression inside a box. The particles have a diameter $d \in [0.6d_{max}, d_{max}]$, with a uniform distribution per volume fraction. Friction, cohesion and gravitational forces are not yet activated. Density ρ_0 of the particles is fixed to $3200kg/m^3$. We extract spherical agglomerates of diameter D from this sample comprising nearly $N_p = 5000$ particles. In order to analyze the effect of aggregate size, four aggregates were built, with $d_{max} \in [3, 6, 12, 18]$m, so D is approximately $[50, 100, 190, 375]$m. Then, the friction coefficient is fixed to 0.4, cohesive forces, modeled as a constant reversible attractive force $-f_0$ with a short range action of the order of $0.01d$, are activated. Gravitational forces are represented by the force $F_{g_0} = \pi d^3 \rho_0 g_0 r/(6D)$ acting on the centre of each particle at a distance r of the centre of the aggregate and pointing towards it. The aggregates are then subjected to diametrical compression between two platens, with a prescribed velocity $V_{wall} = \dot{\gamma} D$ (see Fig. 1(a)). I_η and η were varied between $[5.10^{-4}, 0.1]$ and $[0.1Pa, .., 100MPa]$, respectively. We performed 192 simulations for a broad range of combinations of these two parameters for both, non-gravitational and gravitational aggregates. When gravitational forces are considered, P_0 increases with D, from ~ 0.48Pa, to ~ 30Pa.

During diametrical compression, the vertical stress σ_{zz} acting on an aggregate is given by $4F/\pi D^2$, where F is measured on the platen. It can be also calculated from the micro-mechanical expression of the stress tensor $\sigma_{ij} = n_c \langle f_i^c \ell_j^c \rangle_c$ [27], where $n_c = N_c/V$ with N_c the total number of contact in the volume $V = \pi D^3/6$; the average $\langle ... \rangle_c$ is taken over the contacts c with contact force component f_i^c and branch vector component ℓ_j^c (i.e. the vector joining the centroids of two contacting particles).

Figure 2 shows σ_{zz} as a function of the axial deformation ε_h for $\eta = 1Pa$, $D = 50m$ and different values of I_η, and for $I_\eta = 5 \times 10^{-4}$ with different values of η(inset). ε_h is the classical cumulative vertical deformation defined as $\Delta D/D$ where $\Delta D = D - D_t$ and D_t the height of the wall at the time t. As a general observation, at small I_η values, the stress-strain curve is well defined and has very small deviations around the mean. The stress increases to a peak value at small strain ($\approx$ 2%) before relaxing to a constant plateau (plastic behaviour) at larger strain. Deformations are localized in the vertical plane of the aggregate, where compressive force chains are mainly vertical and tensile force chains lie horizontally (see Fig. 1(b)). This ductile behavior results from particle rearrangements, dissipation due to friction and the short-range action of cohesive forces. As I_η increases, fluctuations in the stress-strain responses increase both in number and magnitude revealing a dynamical crisis. Thus, in the following we consider only results for $I_\eta < 0.035$ for non-gravitational aggregates and $I_\eta < 0.1$ for gravitational ones; the peak stress σ_{zz}^* is defined as an average stress around a deformation of 2%.

In the absence of gravitational forces, we naturally

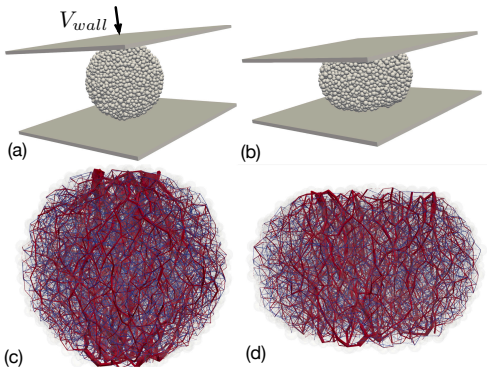

FIG. 1: (Color online) Snapshots of a simulated granular asteroid under diametrical compression for $\varepsilon_h = 0$(a) and $\varepsilon_h = 0.1$(b). Forces chains are represented by lines joining the centres of two touching particles. Compressive forces in red, tensile forces in blue.

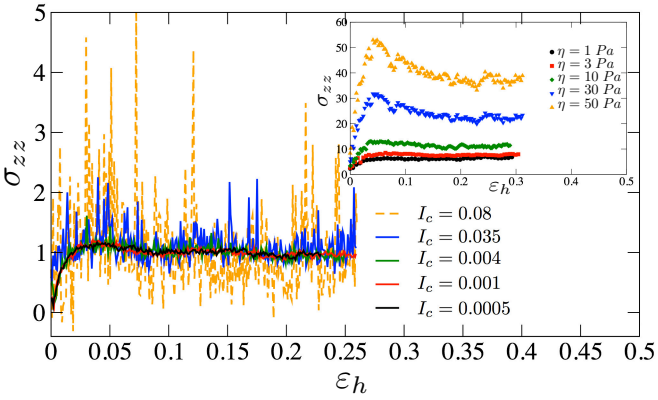

FIG. 2: (Color online) Typical curve showing the vertical strength as a function of the cumulative vertical deformation for $\eta = 1Pa$, $D = 50m$ and various values of I_η (gravitational forces are not activated). The inset show the same curve for $I_c = 5.10^{-5}$, $\eta = \{1, 3, 10, 30, 50\}Pa$ for $D = 190m$ considering gravitational forces.

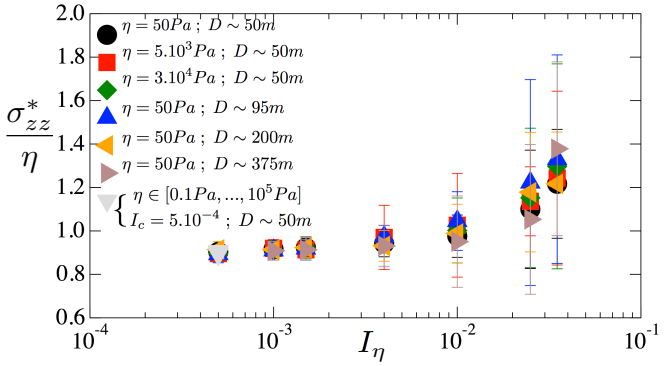

(a)

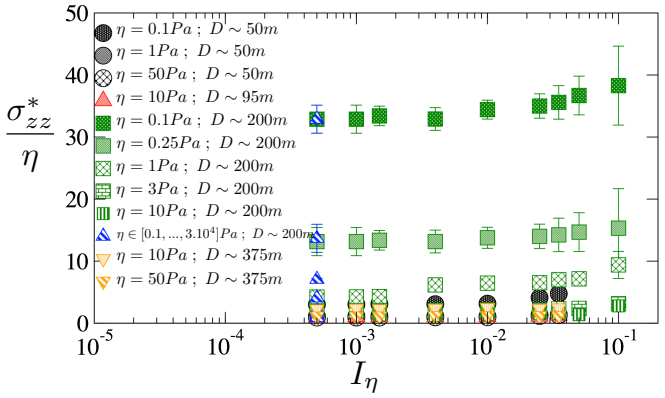

(b)

FIG. 3: (Color online) Peak stress σ^*_{zz} normalized by the cohesive stress η as a function of I_η (a) without gravitational forces (i.e. $I_{g_0} = 0$), and (b) with gravitational forces (i.e. $I_{g_0} \neq 0$), in which only one or two parameters were varied.

expect σ^*_{zz} to scale with η since cohesion is homogeneously distributed in all contacts. This is well observed in Fig. 3(a) for a wide range of values of I_η, η and D. In contrast, when gravitational forces are active, the scaling with η is not verified (see Fig. 3(b)). This is because the effect of gravity is to increase the local stresses acting on the particles, so that interparticle tensile strength and interior stresses become additive. We can thus postulate that the mean pressure is $p = \eta + \alpha P_0$, where α is a weight parameter that represents the stress gradient produced by the radial variation of the gravitational field inside an aggregate. A similar approach has been used for the scaling of shear stresses in dense suspensions [29, 30] and in cohesive granular flow [31], where the fluid or cohesive forces and grain stresses are responsible for the effective friction angle. Accordingly, the inertial number can be re-written as:

$$I' = \dot{\gamma} d \sqrt{\frac{\rho_0}{\eta + \alpha P_0}} = \frac{I_\eta}{\sqrt{1 + \alpha \lambda^{-1}}} = \frac{I_\eta . I_{g_0}}{\sqrt{I_{g_0}^2 + \alpha I_\eta^2}} \quad (1)$$

Figure 4 shows σ^*_{zz} normalized by $(\eta + \alpha P_0)$ as a function of I', for $\alpha = 0.48$. We observe the collapse of all our simulation data with a pre-factor $\simeq 0.9$ for small I' values. This pre-factor (and fluctuations around the mean)

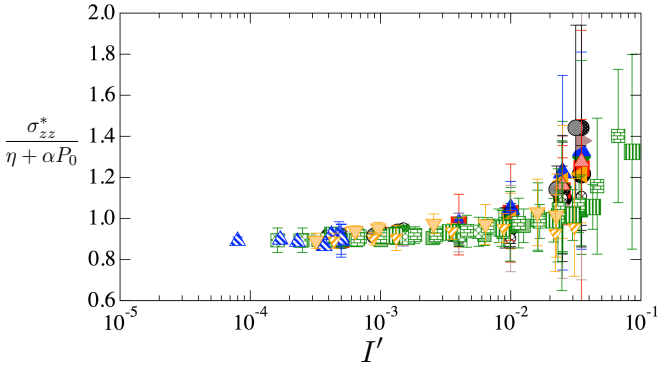

FIG. 4: (Color online) Peak stress σ^*_{zz} normalized by additive stress $p = \eta + \alpha P_0$ as a function of the modified inertial number I' for the raw data (color coding as in Fig 3). Error bars represent the standard deviation around the peak state.

increases with I' to 1.3 in the range of values tested here, evidencing the dynamical crisis resulting from the destabilizing effect of particle inertia. It is thus crucial to explore the extent at which the texture related to the contact and force network is controlled by I'.

At the lowest order, the contact network is characterized by the coordination number $Z = 2N_c/N_p$ (average number of contacts per particle). Much more accurately, the anisotropy of the contact network, evidenced in Fig. 1(b) through a typical representation of forces, is characterized by the probability density functions $P(\boldsymbol{n})$, $\langle f_n \rangle(\boldsymbol{n})$ and $\langle f_t \rangle(\boldsymbol{n})$ of contact normal, mean normal force and mean tangential force, respectively. In 3D, $\boldsymbol{n}$ is defined by the angles (θ, ϕ), but given the spherical geometry of our aggregates, it may be argued that all these distributions are independent of the azimuthal angle ϕ, so in the following, we will consider only the probability densities $P_\theta(\theta)$, $\langle f_n \rangle(\theta)$ and $\langle f_t \rangle(\theta)$ of the radial angles θ (see Fig.5 insets). These distributions are π-periodic and, at the peak state, an approximation based on spherical harmonics at leading terms (only those compatible with the symmetries) can capture their anisotropic behaviour [17, 32]:

$$\begin{aligned} P_n(\theta) &\simeq 1/(4\pi)\{1 + a_c^*[3\cos^2(\theta - \theta_c^*) - 1]\}, \\ \langle f_n \rangle(\theta) &\simeq \langle f_n \rangle\{1 + a_n^*[3\cos^2(\theta - \theta_n^*) - 1]\}, \\ \langle f_t \rangle(\theta) &\simeq -\langle f_n \rangle a_t^* \sin 2(\theta - \theta_t^*), \end{aligned} \quad (2)$$

where $\langle f_n \rangle$ is the mean normal force, a_c^*, a_n^*, and a_t^* are anisotropy parameters, and $\theta_c^* \simeq \theta_n^* \simeq \theta_t^*$ are the corresponding privileged directions which coincide with the major principal stress direction $\theta_\sigma = \pi/2$ in the peak state.

The above microscopic descriptors, calculated in the peak state, are displayed in Fig. 5 as a function of I'. We obtain a very clear collapse of the data points (except maybe for a_n^*), which provides factual evidence for a unified scaling of gravitational and non-gravitational aggregates with the I' formalism. As often observed, a_c^* and Z^* vary oppositely, so the reduction of Z^* with I' repre-

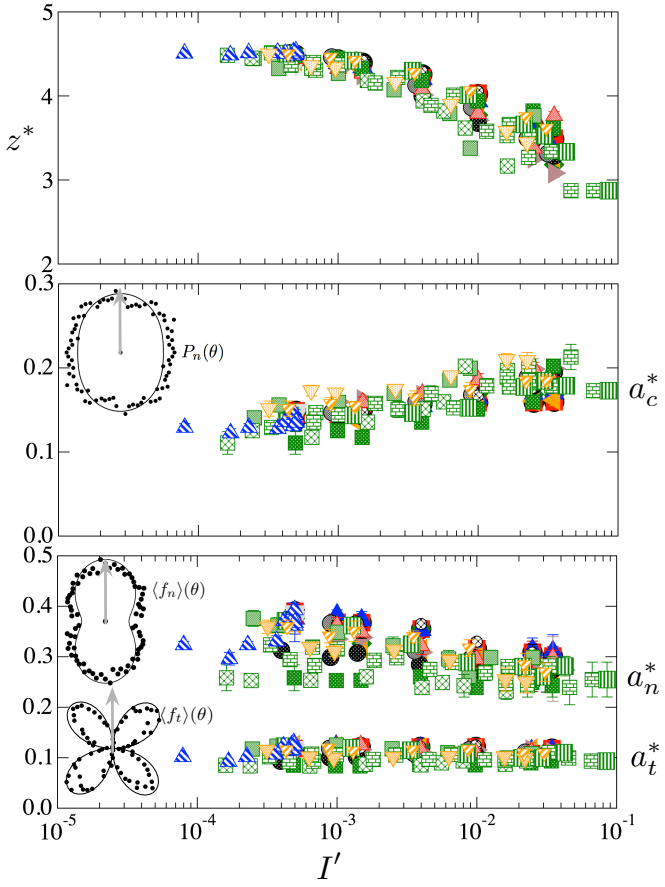

FIG. 5: (Color online) Coordination number Z^* and anisotropies descriptors (a_c^*, a_n^*, a_t^*), as a function of I' (the same color coding as in Fig 3). The inset shows the polar diagrams of the angular distributions (black dot) together with harmonic approximations Eq.2(solid lines) for the smallest I'.

sents the loss of contact in the extension direction [33]. The fact that force chains are increasingly destabilised as I' increases is captured by the decrease of a_n^* together with the fact that a_t, which reflects friction mobilisation ($\langle|f_t|\rangle/\langle f_n\rangle \propto a_t$ [17]), remains constant.

Now, let us remark that the stress tensor can be rewritten as an integral as follows [17, 32]:

$$\sigma_{ij} = n_c \int\int\int f_\alpha \ell_\beta \; P_{\ell f n} \; d\boldsymbol{f} \; d\boldsymbol{\ell} \; d\boldsymbol{n}, \qquad (3)$$

where $P_{\ell f n}$ is the joint probability density of forces and branch vectors $\boldsymbol{\ell} = \ell \boldsymbol{n}$. Neglecting the force-contact correlations (which is numerically always verified), P can be split as $P_{\ell f n} = P_\ell(\boldsymbol{\ell}) P_f(\boldsymbol{f}) P_n(\boldsymbol{n})$. Integrating over $\boldsymbol{f}$ and $\boldsymbol{\ell}$ and considering the normal and tangential components of the forces, we get the following relation [15, 17]:

$$\sigma_{ij} = n_c \ell_0 \int_\Omega [\langle f_n\rangle(\boldsymbol{n}) n_i \langle f_t\rangle(\boldsymbol{n}) t_i] P(\boldsymbol{n}) n_j d\boldsymbol{n}, \qquad (4)$$

where Ω is the angular domain of integration, and $\langle\ell\rangle = \ell_0 \simeq d$ (because of the weak size span [34, 35]). Moreover, it is easy to show that n_c is related to both, Z and the solid fraction $\nu = N_p \pi d^3/(6V)$ by, $n_c = 3Z\nu/(\pi d^3)$ [36]. We assume also that an extreme value of the normal force f_n^* is $(\eta + \alpha P_0)d^2$, on the basis that at the peak state all contacts in a given direction are mobilized in extension and have reached their limit value. In absence of gravitational forces this means that $f_n^* = f_0$. A similar hypothesis, which provided a correct estimate of the strength in direct shearing, was used by Richefeu, et al [36] for wet granular media.

Thus, introducing the expressions of n_c and f_n^* in Eq.4 together with Eq.2, we may introduce a theoretical peak strength for a gravitational aggregate as:

$$\frac{\sigma_{zz}^{theoric}}{\eta + \alpha P_0} = \frac{Z^* \nu^*}{\pi}(1 + \frac{4}{5} a_c^* a_n^*), \qquad (5)$$

where ν^* is the solid fraction at the peak state. Note that this equation can be reduced to the well known "first order" Rumpf's formula for $P_0 = 0$ [37, 38]. For all our simulated data we have $\nu^* \simeq 0.60$. The theoretical values of $\sigma_{zz}^{theoric}$ are shown in Fig. 6 as a function of I', together with those obtained directly from the stress tensor. We observe that Eq. 5 approximates very well the peak stress at low I' values, which explains the microscopic origin of the value of $\simeq 0.90$, but underestimates it at larger values, where impulsive forces prevail, defying the hypothesis done on normal forces at peak state. In the limit of small inertial numbers (i.e. for quasi-static deformation) the important parameters are related to the compactness (solid fraction and number of contacts) and to a lesser extent, to the way in which the contacts and forces are distributed inside the aggregate. Equation 5 provides a clear evidence for the role of these structural parameters for a granular asteroid.

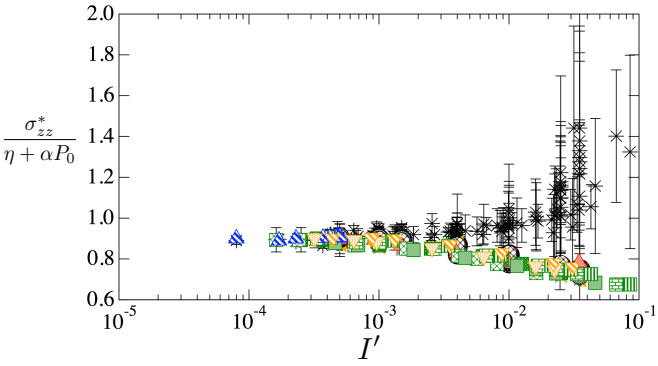

FIG. 6: (Color online) Peak stress σ_{zz}^* normalized by additive stress $p = \eta + \alpha P_0$ as a function of I' for the raw data (stars) same as Fig. 4, together with the prediction given by Eq. 5 (color coding as in Fig. 3).

As explained in the introduction of this article, understanding the physical and mechanical properties of small planetary bodies is an essential step to understand their formation and to plan present and future space missions. One of the outstanding questions in Planetary Sciences was the observation that, though most Near Earth Asteroids (NEAs) had a maximum spin period of ≈ 2.2 h [21],

some of the small members of the population (<150 m) could reach spin periods of just a few minutes. This of course implied that these bodies had an amount of cohesive strength [23, 24] that held them together beyond the gravitational limit; however, no explanation was given to the source of this strength. Prompted by this, [19, 39] proposed that cohesive Van der Waals forces among the small regolith and dust of an asteroid acted as a weak matrix that could hold the larger boulders in place and provide the cohesive strength necessary for the elevated spin rates that had been observed. The specifics of this were explored in [20] arriving to the conclusion that the strength of this matrix was inversely proportional to the average particle radius. This finding, or its principle, has been later used by others [40–42] in their own research. In spite of this, the study of the dynamics of cohesive granular asteroids has been limited to either specific asteroids or to bodies with specific sizes and cohesive strength [43].

To this moment, and even after obtaining a sample from asteroid Itokawa, little is known about the structural strength of small planetary bodies and this was evidenced by the events of the Hayabusa mission to asteroid Itokawa and the Rosseta mission to comet 67P/Churyumov-Gerasimenko. The spacecraft of the Hayabusa mission seems to have touched the surface without piercing it [44] which would imply a cohesive strength of at least some tens of Pascals. These values are in complete agreement with what would be expected if the findings of [20] were applied to a soil formed by mainly micron-size dust and small pebbles. Whereas the lander of the Rosseta mission sank in the regolith of 67/P to then bounce off an underlying more rigid layer which would imply an almost cohesionless upper layer [45].

At this moment, the Hayabusa 2 [46] and OSIRIS-REx [47] missions to asteroids Ryugu and Bennu respectively are scheduled to obtain a sample from their target asteroids. The strength of their surfaces and interiors has been the topic of large research efforts, but they have been focused on the macroscopic strength of the soil disjoint from the global mechanics of the asteroid. The upcoming DART [48] mission is also running into the same question about the strength of asteroid Didymos. Other efforts related to planetary defence and asteroid mining can also be added to the interested parties, but no theoretical explanation has been provided to establish how cohesive and gravitational forces interact to support the structural integrity of granular asteroids or how they scale. This is what we have tried to do with this paper.

The numerical experiments we have carried out do not reflect events that asteroids could undergo; rotational fission, collisions, gravitational tides are not represented by them. However, they allowed us to directly measure characteristics of a self-gravitating aggregate that are independent of the measuring technique. We used an idealised, simpler system that served as a proxy for an asteroid and this is the strength of this work. Given that now we have a theoretical framework, we can explore ways to make our simulations more realistic and applicable to other scenarios. This will be the focus of future research.

To summarize, in this Letter we have defined a consistent framework for the analysis of the behaviour of self-gravitating aggregates, which we used as a proxy for granular asteroids, by extending the I-rheology paradigm. Our extensive numerical simulations provide clear evidence that both macro and microstructure are well captured through a modified inertial number incorporating inter-particle cohesive and gravitational forces. A theoretical model, relating the peak stress to granular texture at sufficiently small I' values, is introduced and shown to be in good agreement with measured data. The present study sheds some new light on a vast and substantial scientific domain given the multitude of open questions related to granular asteroids. The above framework may now be used and extended to analyse much more "complex" self-gravitating systems by incorporating a wide range of particle and asteroid sizes and shapes, and various sources of cohesion (which are generally coupled with particle size [19]) so that they can better represent real asteroids. This will also allow us to explore various dynamical scenarios, such as the rotational evolution of granular asteroids and comets, their reshaping due to planetary tides, or even their exploration, exploitation, redirection or destruction for planetary defence.

Research at the University of Colorado was supported by a grant from NASA's SSERVI program.

[1] V. Badescu, ed., *Asteroids Prospective Energy and Material Resource* (Springer, Berlin, Heidelberg, 2013), ISBN 978-3-642-39244-3, URL https://doi.org/10.1007/978-3-642-39244-3.

[2] R. J. Sullivan, P. C. Thomas, S. L. Murchie, and M. S. Robinson, Asteroids III pp. 331–350 (2002).

[3] M. S. Robinson, P. C. Thomas, J. Veverka, S. L. Murchie, and B. B. Wilcox, Meteoritics and Planetary Science **37**, 1651 (2002).

[4] A. Fujiwara, J. Kawaguchi, D. K. Yeomans, M. Abe, T. Mukai, T. Okada, J. Saito, H. Yano, M. Yoshikawa, D. J. Scheeres, et al., Science **312**, 1330 (2006).

[5] D. Jewitt, J. Agarwal, J. Li, H. Weaver, M. Mutchler, and S. Larson, The Astrophysical Journal Letters **784**, L8 (2014), URL http://stacks.iop.org/2041-8205/784/i=1/a=L8.

[6] D. Jewitt, J. Agarwal, H. Weaver, M. Mutchler, and S. Larson, The Astrophysical Journal Letters **778**, L21 (2013), URL http://stacks.iop.org/2041-8205/778/i=1/a=L21.

[7] H. M. Jaeger and S. R. Nagel, Rev. Mod. Phys. **68**, 1259 (1996), and references therein.

[8] P. Sánchez, Proceedings of the International Astronomical Union **10**, 111 (2015), URL

https://www.cambridge.org/core/article/asteroid-evolution-role-of-geotechnical-properties/CEFD7D6A46A7E74A06F90800DC0E1F6F.

[9] M. Hirabayashi and D. J. Scheeres, The Astrophysical Journal Letters **798**, L8 (2015), URL http://stacks.iop.org/2041-8205/798/i=1/a=L8.

[10] H. Shoucun, J. Jianghui, D.-C. Richardson, Y. Zhao, and Y. Zhang, Monthly Notices of the Royal Astronomical Society **478**, 501 (2018).

[11] R. Delannay, A. Valance, A. Mangeney, O. Roche, and P. Richard, Journal of Physics D Applied Physics **50**, 053001 (2017).

[12] G. D. R. Midi, The European physical journal. E, Soft matter **14**, 341 (2004), ISSN 1292-8941, URL http://www.ncbi.nlm.nih.gov/pubmed/15340859.

[13] F. da Cruz, S. Emam, M. Prochnow, J.-N. Roux, and F. Chevoir, Physical Review E **72**, 021309 (2005), ISSN 1539-3755, URL http://link.aps.org/doi/10.1103/PhysRevE.72.021309.

[14] B. Andreotti, Y. Forterre, and O. Pouliquen, *Granular media: between fluid and solid* (Cambridge University press, 2013), ISBN 9781107034792, URL http://books.google.com/books?hl=en{\&}lr={\&}id=2ekG3NYgpqsC{\&}oi=fnd{\&}pg=PR7{\&}dq=Granular+Media+:+between+fluid+and+Solids{\&}ots=NWzvoVLXE2{\&}sig=dxDaHgET3w7dPaqcBgl6JL3DFd4.

[15] L. Rothenburg and R.-J. Bathurst, Geotechniques **39**, 601 (1989).

[16] F. Radjai, D.-E. Wolf, M. Jean, and J.-J. Moreau, Physical Review Letters **80**, 61 (1998).

[17] E. Azéma, F. Radjai, and F. Dubois, Physical Review E **87**, 062203 (2013), ISSN 1539-3755, URL http://link.aps.org/doi/10.1103/PhysRevE.87.062203.

[18] E. Azéma and F. Radjaï, Physical Review Letters **112**, 078001 (2014), ISSN 0031-9007, URL http://link.aps.org/doi/10.1103/PhysRevLett.112.078001.

[19] D. Scheeres, C. Hartzell, P. Sánchez, and M. Swift, Icarus **210**, 968 (2010), ISSN 0019-1035, URL http://www.sciencedirect.com/science/article/B6WGF-50JHC0F-1/2/cc525a2bf5f1444beab73a75428d8675.

[20] P. Sánchez and D. J. Scheeres, Meteoritics & Planetary Science **49**, 788 (2014), ISSN 1945-5100, URL http://dx.doi.org/10.1111/maps.12293.

[21] P. Pravec and A. W. Harris, Icarus **148**, 12 (2000), ISSN 0019-1035, URL http://www.sciencedirect.com/science/article/pii/S0019103500964820.

[22] K. A. Holsapple, Icarus **154**, 432 (2001), ISSN 0019-1035, URL http://www.sciencedirect.com/science/article/B6WGF-45GWCH0-N/2/c59a8f88823056775eab0aef6baed0c6.

[23] K. A. Holsapple, Icarus **172**, 272 (2004).

[24] K. A. Holsapple, Icarus **205**, 430 (2010), ISSN 0019-1035, URL http://www.sciencedirect.com/science/article/B6WGF-4X3W48Y-1/2/c14b485787c6673f8ccfff09c1047a84.

[25] P.-G. Rognon, J.-N. Roux, M. Naaim, and F. Chevoir, Journal of Fluid Mechanics (2007).

[26] M. Jean, Computer Methods in Applied Mechanics and Engineering **177**, 235 (1999).

[27] J.-J. Moreau, European Journal of Mechanics - A/Solids **13**, 93 (1994).

[28] F. Radjaï and F. Dubois, *Modélisation numérique discrète des matériaux granulaires* (Hermès - Lavoisier, 2010), ISBN 2746229765.

[29] M. Trulsson, B. Andreotti, and P. Claudin, Physical Review Letters **118305**, 1 (2012).

[30] L. Amarsid, P. Mutabaruka, Y. Monerie, F. Perales, and F. Radjai, **012901** (2017).

[31] N. Berger, E. Azéma, J.-F. Douce, and F. Radjai, European physical Letters **112** (2015).

[32] H. Ouadfel and L. Rothenburg, Mechanics of Materials **33**, 201 (2001), ISSN 01676636, URL http://linkinghub.elsevier.com/retrieve/pii/S0167663600000570.

[33] F. Radjai, J.-Y. Delenne, E. Azéma, and S. Roux, Granular Matter **14**, 259 (2012), ISSN 1434-5021, URL http://link.springer.com/10.1007/s10035-012-0321-8.

[34] C. Voivret, F. Radjaï, J.-Y. Delenne, and M. El Youssoufi, Physical Review Letters **102**, 178001 (2009), ISSN 0031-9007, URL http://link.aps.org/doi/10.1103/PhysRevLett.102.178001.

[35] E. Azéma, S. Linero, N. Estrada, and A. Lizcano, Physical Review E **022902**, 1 (2017).

[36] V. Richefeu, M. El Youssoufi, and F. Radjai (2006).

[37] H. Rumpf, Chem.-Ing.-Tech **42(8)**, 538 (1970).

[38] S. Khamseh, J.-N. Roux, and F. Chevoir, Physical Review E **022201**, 1 (2015).

[39] D. P. Sánchez and D. J. Scheeres, Icarus **218**, 876 (2012), ISSN 0019-1035, URL http://www.sciencedirect.com/science/article/pii/S0019103512000292.

[40] M. Hirabayashi, D. J. Scheeres, D. P. Sánchez, and T. Gabriel, The Astrophysical Journal Letters **789**, L12 (2014), URL http://stacks.iop.org/2041-8205/789/i=1/a=L12.

[41] B. Rozitis, E. MacLennan, and J. P. Emery, Nature **512**, 174 (2014), URL http://dx.doi.org/10.1038/nature13632.

[42] E. Tatsumi, D. Domingue, N. Hirata, K. Kitazato, F. Vilas, S. Lederer, P. R. Weissman, S. C. Lowry, and S. Sugita, Icarus **311**, 175 (2018), ISSN 0019-1035, URL http://www.sciencedirect.com/science/article/pii/S0019103517307844.

[43] P. Sánchez and D. J. Scheeres, Icarus **271**, 453 (2016), ISSN 0019-1035, URL http://www.sciencedirect.com/science/article/pii/S0019103516000208.

[44] H. Yano, T. Kubota, H. Miyamoto, T. Okada, D. Scheeres, Y. Takagi, K. Yoshida, M. Abe, S. Abe, O. Barnouin-Jha, et al., Science **312**, 1350 (2006).

[45] J. Biele, S. Ulamec, M. Maibaum, R. Roll, L. Witte, E. Jurado, P. Muñoz, W. Arnold, H.-U. Auster, C. Casas, et al., Science **349** (2015), ISSN 0036-8075, http://science.sciencemag.org/content/349/6247/aaa9816.full.pdf, URL http://science.sciencemag.org/content/349/6247/aaa9816.

[46] S. Van wal, Y. Tsuda, K. Yoshikawa, A. Miura, S. Tanaka, and D. Scheeres, Journal of Spacecraft and Rockets **55**, 797 (2018), URL https://doi.org/10.2514/1.A34157.

[47] D. J. Scheeres and P. Sánchez, Progress in Earth and Planetary Science **5**, 25 (2018), ISSN 2197-4284, URL https://doi.org/10.1186/s40645-018-0182-9.

[48] Y. Yu and P. Michel, Icarus **312**, 128 (2018), ISSN 0019-1035, URL http://www.sciencedirect.com/science/article/pii/S0019103517305328.

[49] We used LMGC90, which is a multipurpose software developed in LMGC laboratory. See https://git-xen.lmgc.univ-montp2.fr/lmgc90/lmgc90_user/